

## ARTICLE

**Delayed Ionization and Delayed Detachment in Molecules and Clusters<sup>†</sup>**

F. Lépine, B. Baguenard, B. Concina, M. A. Lebeault, C. Bordas\*

*Université de Lyon, F-69622, Lyon, France; Université Lyon 1, Villeurbanne; CNRS, UMR 5579, LASIM*

(Dated: Received on January 25, 2009; Accepted on March 23, 2009)

The evolution of a molecular system excited above its ionization threshold depends on a number of parameters that include the nature of the excited states and their couplings to the various continua. The general nature of the processes governing this evolution depends also essentially on the complexity of the molecule, more precisely on its size, density of states, and strength of the couplings among the various internal degrees of freedom. In this paper we address the question of the transition between autoionization that prevails in small molecules, and delayed ionization occurring in larger molecules or clusters. This transition is illustrated by autoionization of Na<sub>2</sub> Rydberg states on one hand, delayed ionization in fullerene C<sub>60</sub>, and delayed detachment in small cluster anions on the other hand. All processes are studied in the case of nanosecond laser excitation, corresponding to a rather slow deposition of the internal energy.

**Key words:** Autoionization, Autodetachment, Thermionic emission**I. INTRODUCTION**

As opposed to the case of simple atomic systems, the photoionization of a molecular system gives rise to a variety of processes owing to the capability of the molecule to accumulate a substantial fraction of its excitation energy in alternative internal degrees of freedom. When a molecule is excited above its ionization threshold, its dynamical behavior depends on the degree and nature of the excitation and on the couplings between its various degrees of freedom. As a general rule, the more complex the molecule is, the less localized on a given degree of freedom the excitation is. This rule is even more appropriate in highly excited molecules where the density of states becomes very high. This is a typical situation where Born-Oppenheimer approximation fails and vibronic couplings become of primary importance for the understanding of the time-dependent behavior of the system. When the excitation energy increases, new decay channels become accessible and compete among each other. From this point of view the study of small gas-phase clusters, and more specifically the study of the decay dynamics of very excited clusters, is a very active field of research [1]. Owing to the combination of relatively simple description and wealth of phenomena that they exhibit, small clusters may indeed be considered as prototypes of finite-size systems that share common properties of small molecules and bulk matter.

In large molecules or clusters the theoretical description of such dynamics becomes untreatable on the microscopic quantum level, in a state-to-state approach. However, this complexity may result in a statistical behavior that can be more simply described within much simpler models [2] that do not necessarily take into account the details of the ongoing processes. The strength of the statistical hypothesis arises from the fact that the system undergoes a dynamics which neither depends on the excitation process nor on its detailed quantum structure but on a few, very general, intrinsic properties such as the number of degrees of freedom, binding energies...

This general behavior has been widely studied especially in the case of delayed ionization of fullerene C<sub>60</sub> [3,4] or delayed detachment in small negatively charged clusters such as refractory metal anion clusters [5]. These processes, which correspond to the release of internal energy by emission of a single electron after a delay ranging from the femto- to the millisecond range, may be valuably studied by photoelectron spectroscopy. In the present paper we will specifically illustrate delayed electron emission in these cases using velocity-map imaging [6,7] that allows recording time-resolved photoelectron spectra giving access to a broad range of emission delay.

The general context of this work is the study of the fate of a molecular system excited above its ionization threshold. In other words the basic question that we are addressing is "how do systems excited above their ionization, or detachment, limit behave?" More specifically we address the question of the phenomena that govern the transition between autoionization and delayed ionization such as illustrated on Fig.1. The small size limit of this process, namely autoionization of Rydberg

<sup>†</sup>Part of the special issue for "the 4th Sino-French Workshop on Molecular Spectroscopy, Dynamics and Quantum Control".

\*Author to whom correspondence should be addressed. E-mail: bordas@lasim.univ-lyon1.fr

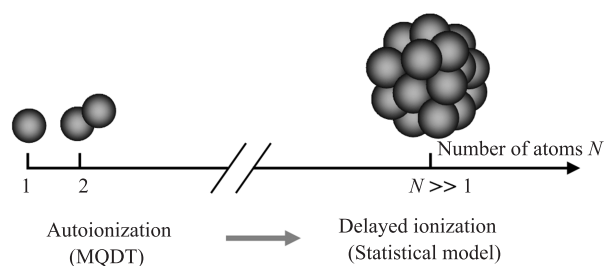


FIG. 1 General scheme of the transition from autoionization in simple atoms or diatomic molecules to delayed ionization in larger molecular systems or clusters. This transition is governed by the interplay between electronic and nuclear motion and depends critically on the size of the systems and above all on its density of states.

states, is abundantly described in Refs.[8,9] and will be briefly illustrated on the particular case of Rydberg states of  $\text{Na}_2$  in the work. Subsequently we will focus on the decay of clusters by electron emission, starting with a short overview of the detailed balance theory [10], the statistical model used to describe delayed emission in large but finite systems, before illustrating these processes by an example of delayed ionization in fullerene and in small metal cluster anions.

When the size of the system increases the density of states becomes so large that two specific characters take place. First the excitation process is no longer resonant and the system can absorb a photon without any kind of selectivity. Second, the couplings between the various internal excitation modes of the system are so large that the timescale for internal couplings is much shorter than the typical time between two photon absorption in the nanosecond excitation regime. Therefore the system can absorb a large number of photons before decaying, the internal energy is redistributed over all degrees of freedom and eventually the system is heated up before decaying. In addition fragments other than electrons may be emitted, but here we focus on cases where the ejected particle is an electron. All these processes may be described within the framework of statistical dynamics, and in case of thermal equilibrium the whole process is designated as thermionic emission.

Basically, autoionization and thermionic or delayed electron emission are the two facets of the same process. In both cases indeed ionization proceeds via an exchange of energy between nuclear and electronic degrees of freedom rather than by a direct ejection of the electron into the continuum. And in both cases also, as opposed to direct ionization which occurs on femtosecond timescale, the ionization or detachment process requires a finite time that can range from the picosecond to the millisecond domain. Understanding the evolution of the interplay between electronic and nuclear motion behind these processes is therefore a fundamental question that raises the question of the transition between these two limiting cases that depends on size, nature of

bindings, and density of states.

## II. MOLECULAR AUTOIONIZATION

The detailed mechanisms of autoionization in atoms or in molecules have been extensively studied in the past. Autoionization is mostly found in atomic or molecular Rydberg states. This has allowed a very specific and very powerful method to be developed to describe the relevant core-electron couplings in full details, namely the multichannel quantum defect theory (MQDT) [11,12]. MQDT is based on the asymptotic form of the Coulomb functions and allows combining the short range properties of the wavefunction included in the quantum defects with the long range asymptotic properties of the Rydberg electron. Therefore it allows a non-perturbative approach that treat on the same footing the structure of the Rydberg spectrum as well as the dynamics of the autoionization process. MQDT was first developed for simple atoms by Seaton [11] and was very rapidly extended to the molecular case by Fano and coworkers [12,13] and subsequently generalized by Jungen *et al.* [14-16] allowing a global description of all kinds of molecular autoionization and dissociation processes. MQDT has also been extensively applied to the case of  $\text{Na}_2$  Rydberg states [17] briefly presented below as an illustration.

Autoionizing states are quasi-discrete states lying above the lowest ionization threshold, members of Rydberg series converging to an excited level of the ion. According to the nature of the excitation of the ion, various kinds of autoionization processes are found. Autoionization involves a non-radiative exchange of energy between the core and the outer electron. The origin of the core energy transferred to the electron may be rotational, vibrational, spin-orbit, or electronic depending on which processes are energetically possible. In a typical molecule like  $\text{Na}_2$ , the most common process is vibrational autoionization. Vibrational autoionization is schematized in Fig.2.

If a Rydberg state of an AB molecule belonging to a series converging towards a  $v \neq 0$  level of the  $\text{AB}^+$  ion lies above the  $v=0$  level of the ion, autoionization occurs by a breakdown of the Born-Oppenheimer approximation. The electronic wavefunction for the quasi-discrete state of the excited neutral is coupled to the one of the ion plus free electron system via the vibronic kinetic energy operator. Autoionization occurs when one ( $\Delta v=1$ ) or several ( $\Delta v>1$ ) quanta of vibration energy in the neutral are converted to kinetic energy of the outer electron, resulting in its ejection. Generally a  $\Delta v=1$  process is much faster than  $\Delta v>1$  processes in a small diatomic molecule like  $\text{H}_2$  [12-16] or  $\text{Na}_2$  [17,18]. This is easily interpreted in terms of vibronic couplings in the framework of MQDT. As a consequence vibrational autoionization favors the emission of slow electrons, with a kinetic energy typically less than one quantum of vi-

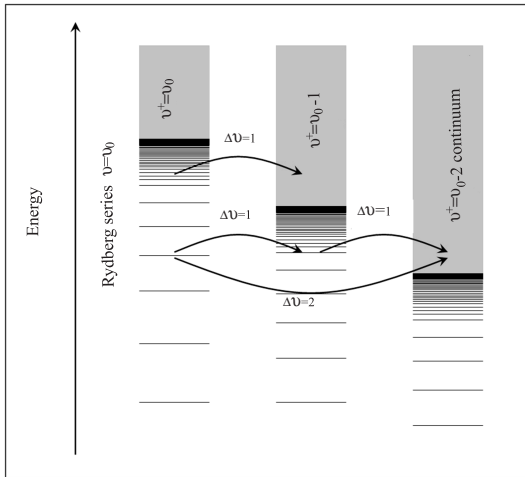


FIG. 2 Schematic illustration of the vibrational autoionization process in a diatomic molecule. Depending on the energy of the Rydberg state the exchange of one or several vibrational quanta is required. In a polyatomic molecule, or in a cluster, the picture of delayed ionization is similar except for the larger number of vibrational degrees of freedom involved, and the correspondingly extremely higher density-of-states.

bration, as compared to emission of fast electrons with large kinetic energy resulting from the exchange of several vibrational quanta with the nuclei. At this point there is of course a significant difference between small diatomic molecules where this propensity rule [19] is almost always verified, and large molecules or clusters where the combination of a large number of degrees of freedom/vibrational modes and large density of states allows rapid couplings among all modes and a fast equilibration of the internal energy over all the accessible energetic modes. The qualitative difference between molecular autoionization and thermionic emission lies precisely in this distinction: molecular autoionization is dominated by  $\Delta v=1$  couplings whereas in larger molecular systems or clusters the strong anharmonic couplings induce a complete mixing that virtually corresponds to a statistical equilibrium among the various degrees of excitation prior to electron emission.

In a small diatomic molecule and at first order the partial linewidth of a given Rydberg state of principal quantum number  $n$  and vibrational quantum number  $v$   $|\Psi_{\ell\lambda,n,v}\rangle$  Rydberg state due to autoionization in the  $v^+=v-1$  continuum when energetically accessible is given by [16]:

$$\Gamma_{\ell\lambda n v; v-1} = 2\pi \frac{2\Re}{n^3} \left( \frac{d\mu_\lambda}{dR} \right)^2 \frac{h}{8\pi^2 m\omega c} v \quad (1)$$

where  $\Re$  is the Rydberg constant,  $m$  is the reduced mass,  $\omega$  is the harmonic vibrational frequency, and  $\mu_{\ell\lambda}(R)$  is the  $R$ -dependent quantum defect defined ac-

ording to:

$$U_{n\ell\lambda}(R) = U^+(R) - \frac{\Re}{[n - \mu_{\ell\lambda}(R)]^2} \quad (2)$$

where  $R$  is the internuclear distance,  $U_{n\ell\lambda}(R)$  is the potential energy curve of the Rydberg state, and  $U^+(R)$  is the potential energy curve of the ion. Keeping only the first order term in the Taylor development of  $\mu_{\ell\lambda}(R)$  and in the harmonic approximation, the only nonzero matrix elements coupling an autoionizing state  $|\Psi_{\ell\lambda,n,v}\rangle$  to the ionization continuum  $|v^+; \varepsilon\rangle$  are those corresponding to  $\Delta v=v^+-v=-1$  that leads to the above first-order expression of  $\Gamma_{\ell\lambda n v; v-1}$ . This very important approximate selection rule is known as the propensity rule of Berry [19]. Within this approximation, the  $\Delta v>1$  matrix elements are zero and autoionizing states of vibrational quantum number  $v$  may be coupled to the ionization continuum  $v^+$  with  $v-v^+>1$  only via indirect couplings involving several  $\Delta v>1$  couplings. Higher order couplings involving higher order dependency of the quantum defect as a function of the internuclear distance are also present but are in general significantly weaker. Therefore, as illustrated in Fig.3, high order vibrational autoionization processes are essentially much slower in small molecules like  $H_2$  or  $Na_2$ .

Vibrational autoionization is induced by an exchange between the kinetic energy of the outer electron and the vibrational energy of the ion core. MQDT allows an explicit and non-perturbative treatment of all rovibrational interactions and includes implicitly all orders of approximation. However, the simpler perturbative approach briefly mentioned above is sufficient in order to emphasize the  $\Delta v=v^+-v=-1$  propensity rule.

As opposed to light molecules like  $H_2$  [12-16] where the dynamics of the autoionizing states is best determined by measuring spectral linewidths, the slower nuclear motion in heavier molecules like  $Na_2$  [17,18] allows the direct observation of the dynamics of autoionization in the time domain as illustrated below.

The sodium diatomic molecule  $Na_2$  chosen to illustrate our discussion has been extensively studied in the past decades [17,18,20]. Sodium molecules are produced as a molecular beam in a thermal oven. The optical excitation is achieved using tunable pulsed lasers (Nd:YAG pumped dye lasers, 10 ns duration,  $0.2 \text{ cm}^{-1}$  spectral linewidth) in an interaction region where a small static electric field (variable from 0.3 V/cm to a few hundreds V/cm) is applied. We follow a selective optical-optical double resonance excitation scheme in order to excite well-defined Rydberg series. The first laser is tuned to a selected rovibrational transition between the ground  $X^1\Sigma_g^+$  and first excited  $A^1\Sigma_u^+$  state. This leads to the selective excitation of the  $Na_2$  molecule in a single  $(v', J')$  level of the intermediate state  $A^1\Sigma_u^+$ . From this intermediate level the second tunable laser is scanned in the vicinity of the ionization threshold. Only Rydberg states of gerade parity with  $J=J'$  or

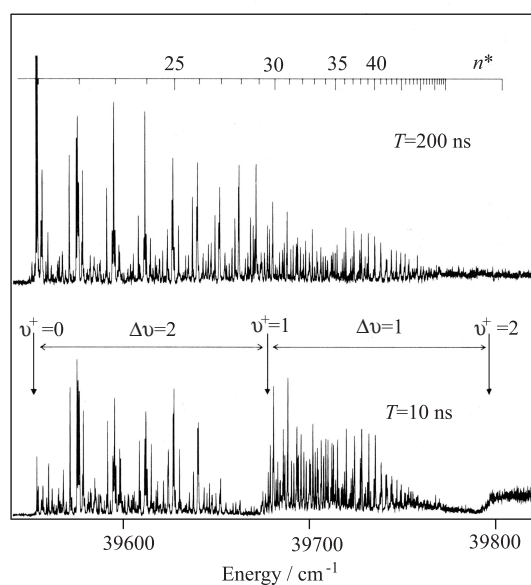


FIG. 3 Experimental spectra of  $\text{Na}_2$  Rydberg states recorded with the intermediate level ( $v'=2, J'=6$ ) for two different integration times (upper spectrum 200 ns, lower spectrum 10 ns). The  $\Delta v=1$  and  $\Delta v=2$  autoionization regions are indicated. Below the direct ionization threshold ( $v^+=2$ ) and the  $\Delta v=1$  ionization threshold ( $v^+=1$ ) lifetimes are noticeably longer. The external electric field ( $F=1.5$  V/cm) is responsible for a well-defined lowering of the ionization thresholds.

$J' \pm 1$  are excited. Owing to the Rydberg character of the A state, the  $v=v'$  Rydberg series are preferentially excited. This allows avoiding congestion of the Rydberg spectra. Typical spectra are found e.g. in Ref.[17,18]. Figure 3 presents the typical behavior of  $\text{Na}_2$  Rydberg states with respect to autoionization. Both spectra presented in this figure have been recorded with the same intermediate level ( $v'=2, J'=6$ ). Only the  $v=2$  Rydberg series is visible in these spectra. The upper spectrum has been recorded using an integration time window of 200 ns (*i.e.* all electrons ejected during the first 200 ns after laser excitation are detected), while the lower spectrum has been recorded with a shorter integration window of 10 ns. The comparison of both spectra gives therefore a direct and qualitative view of the excited states lifetime over a limited range of excitation energy. This method allows a global view of the dynamics based on the fact that the ratio of the relative intensities of similar lines in the two spectra is directly connected to the lifetime of the excited states. Spectra presented in Fig.3 exhibit clearly that the lifetime of autoionizing Rydberg states is typically a few nanoseconds just above the  $\Delta v=1$  autoionization threshold, while it increases to several tens of nanoseconds as  $n$  increases just below the  $v^+=2$  ionization limit. The patterns observed for  $\Delta v=2$  autoionizing states show that lifetime is significantly larger in that case (always larger than 10-20 ns), but show at the same time that the  $\Delta v=1$  propensity

rule is only approximate. Below the direct ( $\Delta v=0$ ) ionization threshold ( $v^+=2$ ) and below the  $\Delta v=1$  ionization threshold ( $v^+=1$ ) the long lifetimes corresponding to vanishing widths are clearly evidenced on the lower spectrum. Note that the various ionization thresholds are lowered by the external electric field (1.5 V/cm).

These results, among others, are symptomatic of the general behavior of molecular autoionization in diatomic molecules. The autoionization lifetime is directly dependent on the precise nature of the excited state and it depends critically on the nature and quantity of energy transferred from the nuclear to the electronic degree of freedom. From this point of view it is clear that the autoionization lifetime does not depend simply on the electron kinetic energy, however it depends very predictably upon the nature of the excited state. The description of the dynamics in the framework of MQDT is of course more subtle than the description of the structure of the Rydberg spectrum but there is no fundamental obstacle to a precise description of the dynamical behavior of every single excited states accessed in this kind of experiment. From this point of view, vibrational autoionization of a small diatomic molecule is therefore anything but statistical.

### III. STATISTICAL DESCRIPTION OF DELAYED IONIZATION IN LARGE MOLECULES OR CLUSTERS

The above description relevant to autoionization in small molecules is no longer true in a cluster where, as noted previously, the high density of states prevents a selective excitation process and induces numerous and stronger couplings between the various degrees of freedom that lead to a very fast redistribution of the internal energy.

Qualitatively, the optical excitation process in the nanosecond regime in a small cluster is very different from the case of a diatomic molecule. The electron-electron couplings timescale are on the order of a few tens of femtoseconds while the e-vibration timescale is in the range of a few hundred femtoseconds. Therefore, if the laser intensity is sufficient, the cluster can absorb an amount of energy substantially larger than its ionization potential or electron affinity as soon as this energy is shared by a large number of degrees of freedom. This property is used in the case of  $\text{C}_{60}$  described below to induce absorption of a large internal energy, typically larger than 50 eV. On the contrary, in the case of small anions with low electron affinity, great care must be taken in order to avoid multiphoton absorption that would induce competing processes (*e.g.* sequential ionization) and very low laser intensity is required. After the absorption of a photon, the very strong couplings among the excited states lead very rapidly to a complete equilibrium and to a thermalization of the system on a femtosecond or picosecond timescale. Therefore, in nanosecond regime, the (multi)photon excitation pro-

cess is equivalent to a heating of the system that lasts over the whole duration of the laser pulse. Hence a statistical approach [2] is relevant to describe “globally” the dynamics of complex systems like clusters or large molecules. In a photoexcited molecular system with an internal energy above the lowest ionization threshold, it may be shown based on simple density-of-states arguments that the coupling of the excited state to other quasi-bound states is in general larger than the direct coupling to the ionization continuum. Due to the strong couplings between the various degrees of freedom, the excitation is no longer localized on a well-defined energetic mode and the internal energy is redistributed in the molecule. In a dynamical picture there is a constant exchange of energy between electronic and nuclear excitation modes. In this picture, the amount of energy in a given degree of freedom fluctuates according to the various couplings. These fluctuations lead to an average equipartition of the energy over all accessible degrees of freedom. They may therefore be described within the framework of statistical mechanics. If at some point the fluctuations are such that the energy accumulated in a given electronic mode exceeds the corresponding ionization limit, electron emission occurs.

When delayed ionization follows the equipartition of the internal energy such as described above, it may be described as a statistical process and is denoted as thermionic emission [21-24]. In order to be efficient as compared to direct ionization, internal energy redistribution must occur rapidly after the initial excitation. From the microscopic point of view, the electron can gain enough energy from the other electrons or from the nuclear motion. In the former case this corresponds to electronic autoionization [25] while in the later case, the amount of energy received by the electron from the nuclei corresponds strictly to the vibrational autoionization process as described above. This correspondence is a characteristic example of the loss of the quantum character of the dynamics of a finite size system, a paradigm of the very general problem of the transition between quantum and classical (statistical) behavior.

Without going into the details, all processes following a statistical redistribution of internal energy may be described in a unified framework which is the detailed balance theory, introduced by Weisskopf in the context of nuclear reactions [10], combined with a proper introduction of the microcanonical temperature(s) [21-23] of the molecule or cluster via the density of states. The detailed balanced theory allows expressing the differential thermionic emission rate as follows:

$$k_{\text{em}}(\varepsilon, E) = \frac{2m}{\pi^2 \hbar^3} \sigma(\varepsilon, E) \varepsilon \cdot \exp\left(\frac{-\varepsilon}{k_B T_d}\right) \exp\left(\frac{-\Phi}{k_B T_e}\right) \quad (3)$$

where  $E$  is the total internal energy,  $\varepsilon$  is the electron kinetic energy,  $\sigma(\varepsilon, E)$  is the electron capture cross-

section of the daughter system,  $\Phi$  is the electron binding energy (ionization potential or electron affinity accordingly), and  $k_B$  is the Boltzmann constant. The parameters  $T_d$  and  $T_e$  are respectively the daughter and emission temperatures, explicit functions of  $E$ . The former is the temperature of the system after electron emission; the later is the mean value of the temperature of the system before and after emission. The differential emission rate appears as the product of terms depending on  $\varepsilon$  that determines entirely the emission spectrum with a term depending only on the emission temperature that determines primarily the total emission rate.

The electron capture cross-section  $\sigma(\varepsilon, E)$  in Eq.(3) may be explicitly estimated via a classical approach [26]. After some approximations, one can derive the following general formula for the thermionic emission spectrum that appears as the product of a simple function of the electron kinetic energy times an exponential term where the important parameter is the daughter temperature  $T_d$ :

$$P(\varepsilon, E) \propto (\varepsilon + C\varepsilon^\gamma) \exp\left(-\frac{\varepsilon}{k_B T_d}\right) \quad (4)$$

The pre-exponential factor consists in two terms. The first one  $\varepsilon$  is given by the contribution of the hard sphere part of the electron capture cross section and vanishes as compared to  $C\varepsilon^\gamma$  when the size of the systems tends to 0. The second term  $C\varepsilon^\gamma$  depends explicitly on the interaction between the electron and the remaining system. Assuming spherical symmetry, one can show that  $\gamma=0$  in the case of a neutral system (delayed ionization) while  $\gamma=1/2$  in the case of an anion (delayed detachment). On the other hand in the bulk limit the hard-sphere contribution dominates and one finds the classical limit of bulk thermionic emission  $\gamma=1$  [27]. The kinetic energy spectrum appears then as a broad distribution and is essentially determined by only two parameters: the temperature  $T_d$  explicit function of the internal energy and related to the density of states, and the exponent  $\gamma$  given by the electron capture cross-section, *i.e.* primarily dependent on the interaction potential between the daughter system and the emitted electron. The total decay rate is simply obtained by integrating Eq.(4) over  $\varepsilon$  and is found as a rapidly increasing function of the internal energy. Characteristic kinetic energy distributions are displayed in Fig.4.

Such emission spectra are characteristic signatures of the statistical character of the delayed ionization in large systems and the precise measurement of the electron kinetic energy distribution is a powerful tool to determine the statistical character of the ongoing process. The detailed characterization of the threshold emission law, qualitatively different from the highly structured spectra observed in the autoionization of small molecules Rydberg states, is therefore the key to unravel the transition between molecular autoionization and thermionic emission.

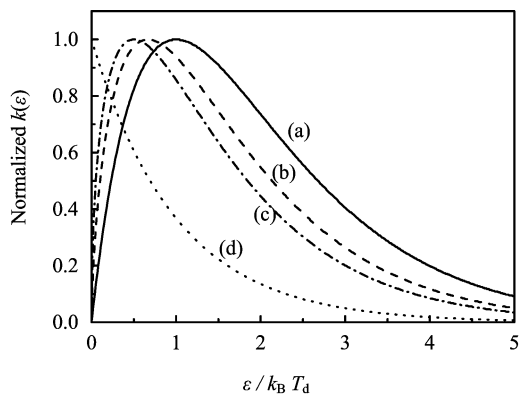


FIG. 4 Generic form of delayed emission spectra as described by Eq.(4). Spectra are displayed in the bulk limit ( $\gamma=1$ )(a) and for three different cases relevant to the small size limit for neutral dissociation ( $\gamma=2/3$ )(b), detachment ( $\gamma=1/2$ )(c), and ionization ( $\gamma=0$ )(d).

Over the past few years, we have developed an experimental set-up allowing the measurement of photoelectron kinetic energy spectra of size selected clusters, at a given time delay after the excitation process. This set-up is based on a velocity map imaging spectrometer [7] with a time-resolved position sensitive detector [28]. In the following section we present the results obtained on delayed ionization of neutral fullerenes and cluster anions using this set-up.

#### IV. DELAYED IONIZATION OF FULLERENE C<sub>60</sub>

As a first illustration of delayed ionization in large molecular systems let us now focus on thermionic emission in fullerene. As far as delayed ionization of finite-size systems is concerned the fullerene C<sub>60</sub> is without any doubt the system that has attracted the largest attention [1,3,4,29,30]. Owing to its high symmetry and large number of degrees of freedom, C<sub>60</sub> has often been used as the paradigm of small systems for studying delayed emission processes both for ionization and for dissociation by emission of C<sub>2</sub> fragments [24]. In the case of thermionic emission in C<sub>60</sub>, Eq.(4) may be explicitly written with  $C=4.1$  eV and  $\gamma=0$ .

The experimental set-up is briefly as follows. A fullerene molecular beam is produced by evaporating C<sub>60</sub> powder in a thermal oven. The multiphoton excitation of the molecules is performed using the third harmonic of a Nd:YAG laser (355 nm, 10 ns duration, 10 Hz repetition rate, variable fluence in the mJ/mm<sup>2</sup> range) in the interaction region. Note that the absorption of more than 10 photons is required to induce delayed ionization on our experimental timescale that ranges between 0 and about 10  $\mu$ s [24]. The interaction between the molecular and laser beams is achieved in a small volume which is simultaneously the center of a velocity-map-imaging (VMI) spectrometer and of

a ion time-of-flight spectrometer. The principle of VMI is very simple [6,7]. A static electric field projects the photoelectrons onto a position sensitive detector made up of a tandem multichannel plate (MCP) followed by a phosphor screen and a CCD camera for read-out. The extraction field is designed such that the position of impact of the electron on the detector depends only on its initial velocity, irrespective of its position, within a finite volume. This device allows the direct measurement of a map of the projection of the electron velocity on a plane perpendicular to the electric field. If the laser polarization is set parallel to the detector plane a simple image inversion [31] provides the electron velocity distribution both in modulus and in direction. In the present case VMI has two main advantages with respect to other photoelectron spectroscopy techniques. First the detection efficiency is independent on the electron kinetic energy and the VMI resolution is very high at threshold. Therefore it is a powerful method for determining threshold spectra. Second, the time of flight of the electron is almost independent on its initial velocity. Hence, by simply gating the microchannel plates detector, one can select a given time slice in the electron distribution and therefore record a delayed emission spectrum in a well defined time window after excitation. The time-resolution of our VMI spectrometer is typically about 50 ns, appropriate to the timescales of the ongoing processes.

For the purpose of studying thermionic emission the suitability of time resolved VMI benefits from the fact that the emission rate describing statistical emission has a very fast (quasi exponential) evolution with the internal energy [24]. This implies that two molecules having a close internal energy have a very different lifetime  $\tau$ . As a consequence the measurement of the electron kinetic energy spectrum at a given time delay  $\tau$  after laser excitation corresponds to the detection of electrons emitted from systems having a rather well defined internal energy  $E$ . A single microcanonical temperature  $T_d(E)$  corresponds to this internal energy. This daughter temperature is experimentally measured by fitting Eq.(4) to the experimental kinetic energy spectrum. These measurements have been published previously [24,32]. A typical example of a delayed photoelectron spectrum recorded in multiphoton ionization of C<sub>60</sub> ( $\lambda=355$  nm, pulse duration=10 ns) is presented in Fig.5 together with the result of the fit according to Eq.(4) where only the temperature  $T_d$  of the residual ion is a free parameter. Indeed for C<sub>60</sub> Eq.(4) may be explicitly written with  $\gamma=0$  and  $C=4.1$  eV. The displayed spectrum has been recorded in a time gate of 1  $\mu$ s width, starting 1  $\mu$ s after laser excitation. Only electrons ejected between 1 and 2  $\mu$ s after excitation are detected, which implies that pure thermionic emission is recorded and the comparison with the statistical model may be performed directly. The experimental spectrum presented in Fig.5 matches perfectly the distribution expected for thermionic emission and this comparison is a

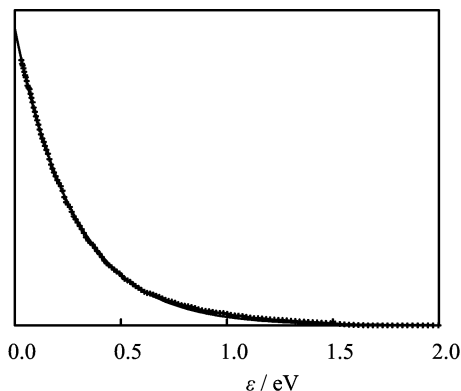


FIG. 5 Delayed ionization of  $C_{60}$ . Photoelectron kinetic energy spectrum recorded at delay  $\tau=1-2 \mu\text{s}$  after the laser excitation (dots). A fitting procedure according to Eq.(4) (line) is used to extract a microcanonical temperature  $T_d^{\text{exp}}=3100\pm 100 \text{ K}$ . This temperature is in excellent agreement with the temperature calculated from the total decay rate  $T_d^{\text{th}}=3180 \text{ K}$ .

representative example of the excellent agreement with the statistical approach. Practically, the photoelectron spectrum may be used as a thermometer to determine the microcanonical temperature of the final product. Since the experimental measurement performed in a well defined time window provides at the same time a precise estimate of the total emission rate this temperature may be compared with the statistical model from this point of view also. The experimental measurement provides also a direct relationship between the total emission rate (via the experimental time-window for detecting the electrons) and the total energy (via the measured temperature  $T_d$ ). As a first approximation, the total ionization rate  $K(E)$  is very often expressed in an simplified Arrhenius form:

$$K(E) = A \exp \left[ -\frac{D_e}{k_B T_e(E)} \right] \quad (5)$$

where  $D_e$  is the dissociation energy required for the ejection of a  $C_2$  fragment (the dominant decay process that governs the total decay rate in the relevant energy range [24]) and  $T_e(E)$  is the corresponding emission temperature. Systematic measurements have been performed for various widths of the integration window between 100 ns and 1  $\mu\text{s}$ , and for delays ranging between less than 100 ns and about 10  $\mu\text{s}$ . Our experimental results are well described using a prefactor  $A=10^{21} \text{ s}^{-1}$  and a dissociation energy  $D_e=10.2 \text{ eV}$  in accordance with the Ref.[33]. For instance, using these values, a very good agreement is found in the particular case of the spectrum displayed in Fig.5 between the experimental temperature  $T_d^{\text{exp}}=3100\pm 100 \text{ K}$  and Eq.(5) that leads to  $T_d^{\text{th}}=3180 \text{ K}$  at delay  $\tau=1 \mu\text{s}$ .

As expected from the statistical approach for a decay process following a full equipartition of the internal energy the experimental spectrum does not present

any discrete structure. On the contrary, all measurements performed at different wavelengths and intensities [24,32] show no significant difference with those presented here, in perfect agreement with the statistical model [10,21-23]. This agreement confirms the statistical nature of delayed ionization in  $C_{60}$ . This is not extremely surprising regarding the size of the fullerene that exhibits a very high density of vibrational states, favoring a rapid equilibrium. In the following section we will focus on smaller systems that do however exhibit a similar behavior.

## V. DELAYED EMISSION IN SMALL TUNGSTEN ANIONS: AUTODETACHMENT AND THERMIONIC EMISSION

As shown in the previous section, delayed ionization of neutral systems appears as a statistical autoionization process where the energy is randomly distributed on the various degrees of freedom leading finally to a more or less efficient coupling with continuum states of the ion+electron system. Anion clusters, despite their different nature (neutral+electron) and the weak long-range interaction between the daughter system and the ejected electron, represent interesting and widely studied species from the point of view of delayed electron emission [34-36]. In our group we have investigated delayed electron emission from anion tungsten clusters  $W_n^-$  [37,38] that represents model refractory systems where electron emission is by far the dominating process with respect to dissociation that is not energetically allowed in the excitation range of interest. Strictly speaking, delayed detachment is no longer an ionization process, however it is similar by many respects to delayed ionization. In particular, as summarized in section III, the same statistical description may be used in that case and the different nature of the interaction potential is entirely taken into account via the exponent  $\gamma$ . An additional advantage of negatively charged systems is that mass selection may easily be performed. This is especially useful in order to investigate the evolution of delayed emission from a small simple system (di- or tri-atomic molecule) to a larger system with many degrees of freedom (like e.g.  $C_{60}^-$ ). From this point of view the study of tungsten cluster anions  $W_n^-$  would allow in principle to follow gradually the transition between a very small system exhibiting discrete structures (autodetachment) and a large system exhibiting a structureless electron kinetic energy spectrum. However, in metal species such as  $W_n^-$ , the DOS is large enough in small clusters (the smaller species obtainable in our set-up is the tetramer  $W_4^-$ ) to induce thermionic emission even in such a small species [37,38].

The experimental set-up is very similar to the one used for neutral fullerenes. A tungsten cluster beam is produced by laser vaporization of a tungsten rod. A pulsed electric field allows extracting native anions

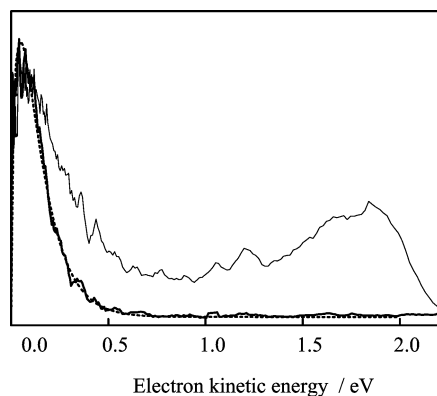


FIG. 6 Photoelectron spectra recorded in one-photon delayed detachment of  $W_{10}^-$  at  $\lambda=308$  nm. Thin solid line: broad integration time-window, direct and delayed electrons are detected. Bold solid line: only delayed electrons are detected in the time window 60-120 ns after laser excitation. A fit of this delayed electron spectrum to Eq.(4) with  $\gamma=1/2$  (dashed line) gives  $T_d=1097\pm 50$  K.

from the molecular beam. A first time-of-flight allows spatial and temporal separation of anions according to their mass. The accelerated anions subsequently enter in the interaction region of a VMI spectrometer. The selection of a well-defined cluster mass is ensured by a proper timing of the excitation laser ( $\lambda=308$  nm, pulse duration=10 ns). Since small cluster anions have a rather low electron affinity (typically below 2 eV) a single photon excitation is sufficient to induce direct or delayed detachment. Therefore, great care is taken in order to avoid multiphoton processes (as opposed to the case of fullerenes) and all experiments are performed at very low laser fluence. Using this experimental set-up, photoelectron spectra of size selected tungsten anion clusters have been measured in the size range between  $n=4$  and 20 [37,38]. Figure 6 illustrates a typical example in the particular case of detachment of  $W_{10}^-$ . Both direct and indirect electron spectra are shown. In the former case, all emitted electrons are detected. In the later, only delayed electrons ejected in a time window 60-120 ns after laser excitation are detected. The delayed electron distribution may be fitted with great precision to Eq.(4) with an exponent  $\gamma=1/2$ , as expected in the case of detachment. Here the  $\varepsilon$  term in the leading factor of Eq.(4) is neglected as compared to  $C\varepsilon^{1/2}$  at threshold. The fit provides a daughter temperature  $T_d=1097\pm 50$  K in good agreement with predictions. A similar agreement is also observed for other cluster sizes ranging between  $n=4$  and 20 [38]. Note that, as quoted previously, even the smallest clusters studied in the present work, namely  $W_4^-$ , exhibits the characteristic features of delayed, statistical, electron emission.

These results, similarly to those obtained for  $C_{60}$ , confirm the statistical character of delayed electron emission in complex systems. Unfortunately, despite

the initial expectations, they do not allow following gradually the transition from quantum to classical behavior since the statistical description is found to be relevant even in the smallest species observed.

## VI. CONCLUSION

The experimental results presented above, first in the case of vibrational autoionization of diatomic molecules, second in the case of delayed ionization or thermionic emission of fullerenes and delayed detachment in clusters, illustrate the evolution of the dynamical properties of finite-size molecular systems of increasing size and complexity. These results illustrate also that this transition from a quantum to a statistical behavior is not necessarily smooth as a function of the size of the molecule and even in a very small system, the exponential increase of the vibrational density-of-states is responsible for a sharp transition towards a statistical character. Although a theoretical description of this transition in a model system is attainable, the detailed experimental characterization of this transition from quantum to classical behavior is more demanding. Moreover it strongly depends on the nature of the system. It is clear for instance that this transition occurs at very small size in metal clusters (e.g. in  $W_4^-$ ) while it may occur at much larger size in complex systems like organic or bio-molecules. Nevertheless, the main conclusion from this work may be the following paradox: the description of autoionization or delayed ionization in a small and simple molecule, within the framework of MQDT for instance, is much more complex and subtle than the description of the same phenomenon in a complex system, where a simple statistical approach allows explaining all observed features. In other words, with the restriction that it is correct only with respect to delayed ionization: complexity makes life easier!

## VII. ACKNOWLEDGMENTS

We warmly acknowledge fruitful discussions with C. Jungen in the early stages of this work. Contributions of M. Broyer, S. Martin, P. Labastie, J. Chevalere, P. F. Brevet, and B. Tribollet to the work on  $Na_2$  Rydberg states are gratefully acknowledged as well as the participation of J. C. Pinaré, F. Pagliarulo, J. B. Wills and B. Climen in the work on fullerene and clusters. We are also grateful to enlightening discussions with K. Hansen and F. Calvo.

- [1] K. Hansen and C. Bordas, *Int. J. Mass. Spectrom.* **252**, (2006).
- [2] W. Forst, *Unimolecular Reactions, a Concise Introduction*. Cambridge: Cambridge University Press, (2003).

- [3] E. E. B. Campbell and F. Rohmund, Rep. Prog. In Phys. **63**, 1061 (2000).
- [4] H. Hohmann, C. Callegari, S. Furrer, D. Grosenick, E. E. B. Campbell, and I. V. Hertel, Phys. Rev. Lett. **73**, 1919 (1994).
- [5] A. Amrein, R. Simpson, and P. Hackett, J. Chem. Phys. **95**, 1781 (1991).
- [6] B. Whitaker, *Imaging in Molecular Dynamics*, Cambridge: Cambridge University Press, (2003).
- [7] A. T. J. B. Eppink, and D. H. Parker, Rev. Sci. Instrum. **68**, 3477 (1997).
- [8] R. F. Stebbings and F. B. Dunning, *Rydberg States of Atoms and Molecules*, Cambridge: Cambridge University Press, (1983).
- [9] M. S. Child, *Molecular Rydberg Dynamics*, Singapore: World Scientific Publishing Company, (2000).
- [10] V. Weisskopf, Phys. Rev. **52**, 295 (1937).
- [11] (a) M. J. Seaton, Proc. Phys. Soc. **88**, 801 (1966);  
(b) M. J. Seaton, Proc. Phys. Soc. **88**, 815 (1966).
- [12] U. Fano, Phys. Rev. A **2**, 353 (1970).
- [13] E. S. Chang and U. Fano, Phys. Rev. A **6**, 173 (1972).
- [14] C. Jungen and O. Atabek, J. Chem. Phys. **66**, 5584 (1977).
- [15] C. Jungen and D. Dill, J. Chem. Phys. **73**, 3338 (1980).
- [16] C. Greene and C. Jungen, Adv. Atom. Mol. Phys. **21**, 51 (1985).
- [17] C. Bordas, P. Labastie, J. Chevalyere, and M. Broyer. Chem. Phys. **129**, 21 (1989).
- [18] P. Labastie, M. C. Bordas, B. Tribollet, and M. Broyer, Phys. Rev. Lett. **52**, 1681 (1984) .
- [19] (a) R. S. Berry, J. Chem. Phys. **45**, 1228 (1966);  
(b) R. S. Berry, Phys. Rev. A **1**, 383 (1970);  
(c) R. S. Berry, Phys. Rev. A **1**, 395 (1970) .
- [20] C. Bordas, P. F. Brevet, M. Broyer, J. Chevalyere, P. Labastie, and J. P. Perrot, Phys. Rev. Lett. **60**, 917 (1988).
- [21] (a) C. E. Klots, J. Phys. Chem. **92**, 5864 (1988);  
(b) C. E. Klots, J. Chem. Phys. **90**, 4470 (1989);  
(c) C. E. Klots, J. Chem. Phys. **98**, 1110 (1993) .
- [22] J. U. Andersen, E. Bonderup, and K. Hansen, J. Chem. Phys. **114**, 6518 (2001) .
- [23] J. U. Andersen, E. Bonderup, and K. Hansen, J. Phys. B **35**, R1 (2002) .
- [24] F. Lépine and C. Bordas. Phys. Rev. A **69**, 053201 (2004).
- [25] M. Raoult, H. Le Rouzo, G. Raseev, and H. Lefebvre-Brion, J. Phys. B **24**, 4601 (1983).
- [26] C. E. Klots, J. Chem. Phys. **100**, 1035 (1994).
- [27] C. Herring and M. H. Nichols, Rev. Mod. Phys. **21**, 185 (1949) .
- [28] B. Baguenard, J. B. Wills, F. Pagliarulo, F. Lépine, B. Climen, M. Barbaire, C. Clavier, M. A. Lebeault, and C. Bordas, Rev. Sci. Instr. **75**, 324 (2004).
- [29] D. Ding, R. N. Compton, R. E. Haufler, and C. E. Klots, J. Phys. Chem. **97**, 2500 (1993).
- [30] E. E. B. Campbell, K. Hansen, K. Hoffmann, G. Korn, M. Tchapyguine, M. Wittmann, and I. V. Hertel, Phys. Rev. Lett. **84**, 2128 (2000).
- [31] C. Bordas, F. Paulig, H. Helm, and D. L. Huestis, Rev. Sci. Instr. **67**, 2257 (1996).
- [32] F. Lépine, B. Climen, F. Pagliarulo, B. Baguenard, M. A. Lebeault, C. Bordas, and M. Hedén, Eur. Phys. J. D **24** 393 (2003).
- [33] S. Tomita, J. U. Andersen, K. Hansen, and P. Hvelplund, Chem. Phys. Lett. **382**, 120 (2003).
- [34] H. Weidele, D. Kreisle, E. Recknagel, G. Schulze Icking-Konert, H. Handschuh, G. Ganteför, and W. Eberhardt, Chem. Phys. Lett. **237**, 425 (1995).
- [35] G. Ganteför, W. Eberhardt, H. Weidele, D. Kreisle, and E. Recknagel, Phys. Rev. Lett. **77**, 4524 (1996).
- [36] C. E. Klots and R. N. Compton, Phys. Rev. Lett. **76**, 4092 (1996).
- [37] J. C. Pinaré, B. Baguenard, C. Bordas, and M. Broyer, Phys. Rev. Lett. **81**, 2225 (1998).
- [38] B. Baguenard, J. C. Pinaré, C. Bordas, and M. Broyer, Phys. Rev. A **63**, 023204 (2001).